Quarterly Progress Report

on

Configurational Diffusion of Coal Macromolecules

James A. Guin
Christine W. Curtis
A. Ray Tarrer

Auburn Coal Conversion Laboratory
Chemical Engineering Department
Auburn University
Auburn, AL 36849

Table of Contents

Acknowledgements

The work reported herein was made possible by the efforts of the following personnel of the Auburn Coal Conversion Laboratory. Their contributions to this report and to the progress of this work are hereby gratefully acknowledged.

Seongjae Kim

Frank Bowers

Objective and Task Outline

Objective

To investigate the phenomenon of hindered diffusion of coal macromolecules in idealized porous media.

Task Outline

Task 1. Construct a diffusion cell with ideal pore structure for determination of diffusion coefficients.

Task 2. Prepare and characterize ideal porous membranes.

Task 3. Perform model compound experiments to calibrate and test diffusion apparatus and methodology.

Task 4. Prepare and characterize coal macromolecules.

Task 5. Analyze data to evaluate the diffusional behavior of coal macromolecules.

List of Figures and Tables

Figures

Tables

Summary of Progress

During this quarter, the results of hindered diffusion experiments with tetraphenylporphine (TPP) and coal macromolecules were evaluated in the light of the hindered diffusion theory. Statistical methods were used to examine the significance of departure of the experimental data from the theoretical curve predicted by the hindered diffusion theory.

The statistical studies showed that the differences between the experimental data and theoretical curve for both experimental sets (TPP diffusion and coal macromolecules diffusion) were significant. Weak attractive interactions between TPP molecules transferring through the pore and the pore wall were postulated to account for the slightly weaker hinderance effects compared to the theoretical curve observed in TPP diffusion data, while weak repulsive interactions between adsorbed coal molecules and the ones diffusing through the pore were speculated to explain the stronger hinderance effects in coal diffusion data.

1. Hindered Diffusion of Tetraphenylporphine (TPP)

Introduction

Details of the hindered diffusion experiments for TPP were described in the previous reports (1,2). In this report, an evaluation of experimental results will be discussed.

Results and Discussion

In Table 1, the experimental results of bulk diffusion coefficient measurements are summarized along with the estimated value. The estimated values for the diffusion coefficient of TPP in ethyl acetate were calculated from the diffusion coefficient of TPP in chloroform at 20 °C reported by Anderson et al. (3) They reported that the diffusivity of TPP was 5.75×10^{-6} cm^2/sec. To estimate the diffusivity of TPP in ethyl acetate at 25 °C from this value, the Wilke-Chang equation was used as shown in Table 1. The experimental value (6.83×10^{-6} cm^2/sec) was about 10 percent greater than the estimated value (6.17×10^{-6} cm^2/sec). The Stokes-Einstein radius of TPP obtained from the experimental bulk diffusion coefficient was 7.24 Å.

The results of the hindered diffusion experiments of TPP are presented in Figure 1, where D_{eff}/D_∞ is plotted against r_s/r_o (λ). The solid line in this curve is drawn from the theory proposed by Anderson et al. (3) for the hindered diffusion of thin disk-shaped molecules. The equation is expressed as:

$$\frac{D}{D_\infty} = (1 - (\frac{\pi^2}{8})\,\lambda)^2 \,(1 - 2.1044\,\lambda + 2.088\,\lambda^3 - 0.948\,\lambda^5) \quad (1.1)$$

2

As shown in Figure 1, it appears that the hindered diffusion data fall slightly above this theoretical curve. To clarify this observation, several statistical methods were used to examine the significance of the difference between the experimental data and the theoretical curve. The results of the statistical studies are summarized in Table 2.

Two nonlinear curve-fitting methods in the table had been used in several previous hindered diffusion studies (4,5,6), whereas the other curve-fitting method was a second degree polynomial regression. For each curve-fitting method, the parameters of the theoretical curve were obtained by using 300 theoretical data points ranging from 0.0 to 0.3 calculated from Equation 1.1. As shown in this table, the parameter from the theoretical data is outside the 99% confidence level limits of the model parameters for the two nonlinear fittings from the experimental data. Differences between theoretical and experimental data also can be seen in the second degree polynomial regression. Probabilities of hypothetical tests for closeness between the theoretical and experimental polynomial coefficients are almost zero.

Results obtained from this study are also different from the findings of the hindered diffusion study of TPP with chloroform using a track-etched mica membrane reported by Anderson et al. (3). Their experimental data were in excellent agreement with the theoretical predictions.

The reduction in diffusivity of solute in the hindered diffusion experiment is due to two factors: the partitioning effect and the frictional effect. The first bracket of Equation 1.1 represents the partitioning effect term, while the second bracket represents the frictional effect term.

The expression for the frictional effect in Equation 1.1 had been derived for the movement of a rigid spherical solute in a cylinder by using the "centerline approximation" (the sphere on the cylinder's centerline). Since the molecule used in the current study was a rigid disk-shaped molecule, this approximation might produce an error in the theoretical curve. However, the approximate expression used in Equation 1.1 has been used successfully in many previous hindered diffusion studies by implementing the hydrodynamic radius calculated from the Stokes-Einstein equation. Also, use of the centerline approximation underestimated the frictional factor. Thus, it appeared that the differences observed in Figure 1 were not caused by using the approximate equation derived for the hard sphere.

A more rigorous treatment concerning the mobility factor of this molecule in a cylindrical pore might be required to evaluate the experimental results. However, this kind of approach was not available in the literature to date.

Compared to the frictional factor, the partitioning coefficient term has been studied quite extensively for the various shapes of molecules in differently shaped pores (7,8,9). The partitioning coefficient term is the equilibrium ratio of

pore to bulk concentration of solute. The general expression for the partitioning coefficient of arbitrary shape of molecule in an arbitrary pore is:

$$K_p = \frac{\iiint \exp(-E_p(\zeta, v, \xi)) \, d\zeta \, dv \, d\xi}{\iiint \exp(-E_b(\xi)) \, d\zeta \, dv \, d\xi} \qquad (1.2)$$

Here ζ, v, and ξ are the general coordinates describing molecular position, orientation and conformation, respectively. E_p and E_b are the interaction potentials of the molecule in the pore and bulk. This equation can be written in a more simplified form with the following considerations: (1) the solute is a rigid molecule, i.e., only a single conformation exists; and (2) the solution is infinitely dilute, and thus is ideal. Equation 1.2 becomes:

$$K_p = \frac{\iint \exp(-E(\zeta, v)) \, d\zeta \, dv}{\iint d\zeta \, dv} \qquad (1.3)$$

Here, E is the interaction potential between the solute molecule and the pore wall. The physical interactions between the solute and pore wall are usually the result of the attractive or repulsive Van der Waals forces or repulsive electrostatic interactions (E<0). As previously discussed, if E=0, then the partition coefficient represents only the steric effect. For the sphere in a cylindrical pore with pure steric interaction, Equation 1.3 becomes:

$$K_p = \left(1 - \frac{a}{r_o} \right)^2 \qquad (1.4)$$

For the spherical solute, the radius of the molecule is the same as the Stokes-Einstein radius. However, for the rigid disk-shaped molecule, another molecular length scale representing the orientation and size should be used as shown in Equation 1.3.

Giddings et al.(7) found that the use of the mean external (projected) length to describe the partitioning behavior of nonspherical molecules was better than the use of any other measure of molecular size. The mean projected length for the axisymmetric molecule is defined as:

$$X_m = \int_0^{\frac{2}{\pi}} h(\theta) \sin\theta \, d\theta \qquad (1.5)$$

where h is the closest approach length of the center of the molecule and θ is the angle between the axis of the molecule's rotation and the unit normal vector of molecules.

Baltus (8) reported the following expression relating the Stokes-Einstein radius to the mean projected length for disk-shaped molecules by combining Gidding's expression for the mean projected length and Happel and Brenner's work (10) for the effect of the hydrodynamic radius of the disk-shaped molecule.

$$\frac{X_m}{r_s} = \frac{\sin^{-1}(1-\phi^2)^{0.5}}{(1-\phi^2)^{0.5}} \left[\frac{\phi}{2} + \frac{\sin^{-1}(1-\phi^2)^{0.5}}{2(1-\phi^2)^{0.5}} \right] \qquad (1.6)$$

Here, ϕ is the ratio of minor-to-major axis. As the value of ϕ approaches zero, the value of X_m/r_s in Equation 1.6 becomes the asymptotic value, $\pi^2/8$. The expression in the first bracket of Equation 1.1 was obtained from the aforementioned process.

Since TPP has a certain thickness because of π-electrons, the ϕ value is greater than zero. In Figure 2, the theoretical

curves with different ϕ values are presented along with the TPP hindered diffusion experimental data. As shown in this figure, the introduction of the ϕ parameter in the theoretical curve still does not explain the differences between the experimental data and the theoretical curve.

The only term which was not considered up to this point was the interaction between solutes and pore walls. The use of Equation 1.1 assumes that there are no solute-pore wall interactions. However, if the attractive interaction energy is introduced to the theoretical curve as shown in Equation 1.3, the partition coefficient increases, and the theoretical curve for D_{eff}/D_{∞} thus moves in the experimental data points' direction (upward).

As Deen (9) pointed out in his review paper on hindered diffusion, few studies have been conducted previously concerning the characterization of solute-pore wall interactions, especially attractive forces. However, a simulation study concerning the partitioning of a polymer with attractive interactions conducted by Davidson et al. (10) using a Monte Carlo simulation technique showed that the partitioning coefficient increased substantially when moderate attraction energy was included.

Since our experimental data fell slightly above the theoretical curve, the result indicated that weak interactions occurred between TPP and the pore walls of polyester membranes.

In comparing the current experimental results with the TPP hindered diffusion experimental results conducted by Anderson et

al. (3), their experimental data almost fell on the theoretical curve; thus, the concept of attractive interaction was not required to evaluate their experimental data. The solute-pore wall interactions are the result of complex interactions: between solute and pore wall, between solvent and pore wall, and between solute and solvent. Since their experimental system was different from that used in the current study (e.g., track-etched mica membrane /polyester membrane, chloroform/ethyl acetate), TPP might experience different interactions in the current study. One thing to be noted in their experiment is that the shape of mica membrane pore opening was rhombohedral. This fact leads to some ambiguity in defining an "equivalent" circular pore, since theoretical equations are not available for rhombohedral pores.

2. Hindered Diffusion of Coal Macromolecules

Introduction

Details of experimental results for the hindered diffusion of coal macromolecules were also described in the previous reports (1,2). In this section, results of statistical study and an evaluation of experimental results will be discussed.

Results and Discussion

In Table 3, the measured bulk phase diffusivities for coal macromolecules' fractions are summarized. In the analyses of experimental data to calculate the bulk diffusivities of coal macromolecules, the hinderance factor of each coal fraction was taken into account. As shown in this table, the bulk diffusivities decreased as the equivalent molecular weights of coal molecules increased. The standard deviations of bulk diffusivities were somewhat large compared to those of model compounds' diffusivities. These relatively large experimental errors appeared to be due to the errors in GPC analysis and the errors associated with the charging of the stock solution to the diffusion cell.

In Figure 3, the ratios of effective diffusivities to bulk diffusivities are plotted against the ratios of molecular sizes to the average pore sizes. Here, the molecular size of each coal fraction was calculated from the bulk diffusivity by using Stokes-Einstein equation ($r_s = k \cdot T / (6\pi \cdot \mu \cdot D_\infty)$). The solid line drawn in Figure 3 represents the theoretical data calculated from

9

Equation 1.1. As shown in this figure, the experimental data
fall below the theoretical curve. The results were somewhat
contrary to that of TPP, where experimental data fell above the
theoretical curve. In order to evaluate the significance of the
deviation between the experimental data and the theoretical
curve, the same statistical methods used to evaluate the
experimental results of TPP were carried out.

The results are summarized in Table 4. The model parameters
for the theoretical curve were the same as those obtained
previously. As shown in this table, all statistical studies
indicated that significant differences existed between the
theoretical curve and the experimental data. In order to explain
these differences, it should be noted here that the pore
diameters of membranes decreased during the hindered diffusion
experiments of coal macromolecules. It should also be noted here
that the true pore radii values obtained from the in situ
diffusivity measurement of n-octane were used in Figure 3. As
described previously (2), it was surmised that the change in pore
diameters was due to the adsorption of coal molecules to the pore
walls. This hypothesis becomes apparent when the chemistry of
coal asphaltene is examined more closely. According to the coal
asphaltene model proposed by Yen (11), coal asphaltene
interestingly has the acidic and basic nature. The acid-base
structure of coal asphaltene was also demonstrated by
Sternberg et al. (12). They separated the coal asphaltene into
acid-neutral components and base fractions by dissolving the

asphaltene in toluene and passing dry HCl gas through the solution. The basic component was precipitated as an insoluble adduct while the acidic and the neutral components remained in the solution. The authors reported that the expected functional groups in the acidic components were phenolic O-H and pyrrolic N-H, while those in the basic components were ring oxygen as in furan or ring nitrogen as in pyridine; these components were responsible for the hydrogen bonding. They thought that the acidic and the basic components were separately solvated in solvents such as benzene. The acid-base structure of coal asphaltene was also proved by Sidney et al. using infrared spectrometry (13).

Although the model of coal asphaltene structure studied in these works did not quite agree with the model proposed by Yen, both models acknowledged the existence of hydrogen bonding between acidic and basic functional groups in coal asphaltene.

All of the aforementioned studies implied that either acidic or basic components (or functionalities) of coal asphaltene solvated in ethyl acetate might selectively adsorb to the pore walls of membranes in the current hindered diffusion experiments. These adsorbed molecules were likely to interact with other coal molecules transferring through the pore; these interactions were expected to be an electrostatic repulsive interaction. The degree of interactions would not be strong because of the low concentration used in the current study, as well as the characteristics of coal asphaltene (e.g., the existence of

neutral components according to Sternburg et al.'s study).

Nevertheless, this repulsive interaction could decrease the partition coefficient, thus making the experimental data fall below the theoretical curve derived with the no pore-molecule interaction assumption.

The effect of electrostatic repulsive interactions on the partition coefficient has been investigated in several previous studies (14-17). Among these studies, the experimental study conducted by Rodilosso drew attention because of the phenomenal similarity found in his experimental results and the current study. He measured the partition coefficient for bovine serum albumin (BSA, $r_s \approx 36\text{Å}$) in a track-etched mica membrane which had pore walls precoated with BSA by adsorption (experimental conditions: dilute solution of BSA at pH 8.5 and 0.2 M ionic strength). He reported that the partition coefficient was found to be at least one order of magnitude lower than the theoretical curve obtained from simple steric exclusion; he explained that these observations were due to the electrostatic repulsive interactions between BSA molecules in the solution and the BSA-coated pore wall. The nature of the electrostatic interactions found in his study might be different from those observed in the current research since most protein molecules were charged depending on the pH of the solution. However, it was apparent that the interactions between adsorbed molecules and transferring molecules through the pore decreased the partition coefficient, and that these interactions were due to the existence of

functional groups in the molecules. All of these findings
support the hypothesis used to explain the phenomenon observed in
Figure 3.

Before any final conclusions concerning the observations
seen in the hindered diffusions of coal macromolecules are made,
relatively large experimental errors found in the bulk
diffusivity measurements should be discussed. As seen in Table
3, the standard deviations of bulk diffusivity value reached
about 10%. Experimental errors also existed in the effective
diffusivity measurements. In Figure 3, the lines connecting two
points represent the experimental data obtained from two
consecutive hindered diffusion experiments conducted with the
same polyester membrane. As seen in this figure, experimental
data points were not completely reproducible. Again, it was
suspected that these experimental errors were due to the errors
in GPC analysis.

These experimental errors could be large enough to mask the
differences between the experimental data and the theoretical
curve observed in Figure 3. However, it is the scatter of
experimental data that is affected by experimental errors. As
seen in Figure 3, the current experimental data do not scatter
randomly around the theoretical curve. They scatter below the
theoretical curve and the significance of deviation from
theoretical curve was already examined by the statistical
methods. Thus, it is likely that the conclusion drawn relating
to electrostatic repulsion is the reason why the coal

macromolecules are more hindered than predicted by the neutral hard sphere theory.

References

1. <u>Quarterly Progress Report</u>, Mar. 15, 1990

2. <u>Quarterly Progress Report</u>, Jun. 15, 1990

3. Anderson, J. L., Kathawalla, I. A. and Lindsey, J. S., <u>AIChE Symposium Series 266</u>, (84), 35, 1988

4. Beck, R. E. and Schultz, J. S., <u>Biochim. Biophys. Acta</u>, (255), 273, 1972

5. Satterfield C. N., Colton, C. K. and Pitcher, Jr., W. H., <u>AIChE J.</u>, (19)3, 628, 1973

6. Baltus, R. E. and Anderson, J. L., <u>Chemical Engineering Science</u>, (38)12, 1959, 1983

7. Giddings, J. C., Kucera, E., Russell, C. P. and Myers, M. N., <u>J. Phys. Chem.</u>, 72, 4392, 1988

8. Baltus, R. E., <u>Macromolecule</u>, 22, 1775, 1989

9. Deen, W. M., <u>AIChE J.</u>, (33)9, 1409, 1987

10. Davidson, M. G., Suter, U. W., and Deen, W. M., <u>Macromolecule</u>, 20, 1141, 1987

11. Yen, T. F., <u>Coal Chemistry Workshop</u>, Aug. 26-27, Monlo Park, California, 1976

12. Sternberg, H. W., Raymond, R. and Schwighardt, F. K. <u>Science</u>, 188, 49, 1975

13. Sidney, F. B., MAkovsky, F. L. and Schweighardt, F. K., <u>Applied Spectroscopy</u>, 31(3), 241, 1977

14. Malone, D. M. and Anderson, J. L., <u>AIChE J.</u>, (23)2, 177, 1977

15. Smith III, F. G. and Deen, W. M., <u>J. of Colloid and Interface Science</u>, 91(2), 571, 1983

16. Smith III, F. G. and Deen, W. M., <u>J. of Colloid and Interface Science</u>, 98(2), 444, 1983

17. Rodilosso, P. D. <u>Ph.D. Thesis</u>, University of Pennsylvania, 1984

18. <u>Quarterly Progress Report</u>, Dec. 15, 1989

Table 1

Measurements of the Bulk Diffusion Coefficient of TPP in Ethyl Acetate @ 25°C.

Membrane No.	# of Obs.	Measured Value $(cm^2/sec \times 10^6)$	Estimated[a] Value $(cm^2/sec \times 10^6)$
CPE2001	3	6.90 ± 0.10	
CPE2002	3	6.77 ± 0.13	
Average	6	6.83 ± 0.13	6.17

a. Estimated from the value reported in ref. 3 and Wilke-Chang equation, i.e.

$$D_{\infty 1} = D_{\infty 2} (T_1/T_2)(\mu_2/\mu_1)(M_1/M_2)^{0.5}$$

Table 2

The Results of Statistical Tests for the
Hindered Diffusion Data of TPP

Curve Fitting Model[a].	Parameter From Theo. Data	Parameter From Expr. Data	95% Confidence Level Limit of Parameters(exp.)	99% Confidence Level Limit of Parameters(exp.)
$Y=(1-X)^z$	$Z=4.833$	$Z=4.25$	$3.99<Z<4.51$	$3.91<Z<4.59$
$Y=e^{-kx}$	$k=5.33$	$k=4.53$	$4.25<k<4.82$	$4.16<k<4.91$
2nd Order Polynomial Regression[b].	$a_1=-4.458$ $a_2=5.688$	$a_1=-3.501^{c.}$ $a_2=0.4746$		

a. $Y=D_{eff}/D_\infty$, $X=r_s/r_o$.
b. $Y=i+a_1X+a_2X^2$.
c. F-test result of a_1 from experiment equals a_1 from theoretical data: Prob>F :0.006,
F-test result of a_2 from experiment equals a_2 from theoretical data: Prob>F :0.0037.

Table 3

Bulk Diffusion Coefficients of Coal
Asphaltene Fractions

Fractions (elution volume(ml))	Equivalent[a] M. Wt (g/mole)	Diffusion[b] Coefficients $cm^2/sec) \times 10^6$	Stokes Einstein Radius(Å)[c]
25 - 27	1237	4.19 ± 0.44	11.8
27 - 29	ᵒ⌐6	5.53 ± 0.62	9.0
29 - 31	739	6.78 ± 0.50	7.3
31 - 33	570	7.87 ± 0.56	6.3
33 - 35	440	8.62 ± 0.70	5.7
35 - 37	340	9.22 ± 0.76	5.4

a. Molecular weight estimated from GPC calibration curve (18)
b. No of observations : 10.
c. The radii were determined from Stokes-Einstein
    equation $(D_a = k \cdot T/(6\pi \cdot \mu \cdot a))$.

Table 4

The Results of Statistical Tests for the Hindered
Diffusion Data of Coal Macromolecules

Curve Fitting Model[a].	Parameter From Theo. Data	Parameter From Expr. Data	95% Confidence Level Limit of Parameters(exp.)	99% Confidence Level Limit of Parameters(exp.)
$Y=(1-X)^z$	$Z=4.83$	$Z=7.09$	$6.84<Z<7.33$	$6.76<Z<7.41$
$Y= e^{-kx}$	$k=5.33$	$k=7.54$	$7.28<k<7.79$	$7.20<k<7.87$
2nd Order Polynomial Regression[b].	$a_1=-4.458$ $a_2= 5.688$	$a_1=-6.973$[c]. $a_2=15.7692$		

a. $Y=D_{eff}/D_e$, $X=r_s/r_o$.
b. $Y=1+a_1X+a_2X^2$.
c. F-test result of a_1 from experiment equals a_1 from
   theoretical data: Prob>F :0.0001.
   F-test result of a_2 from experiment equals a_2 from
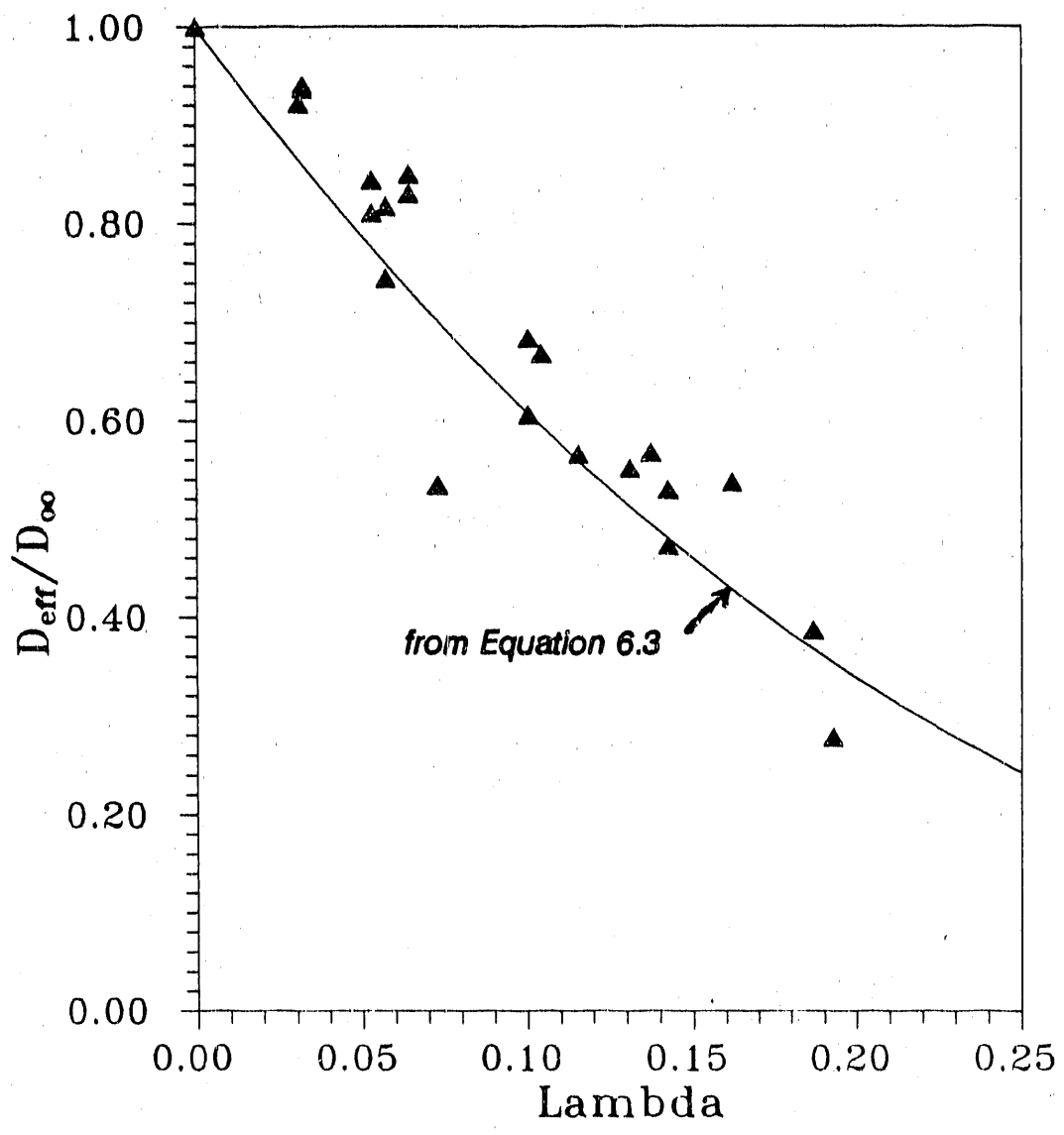   theoretical data: Prob>F :0.0001.

Figure 1 Dependence of D_{eff}/D_∞ on λ in Hindered
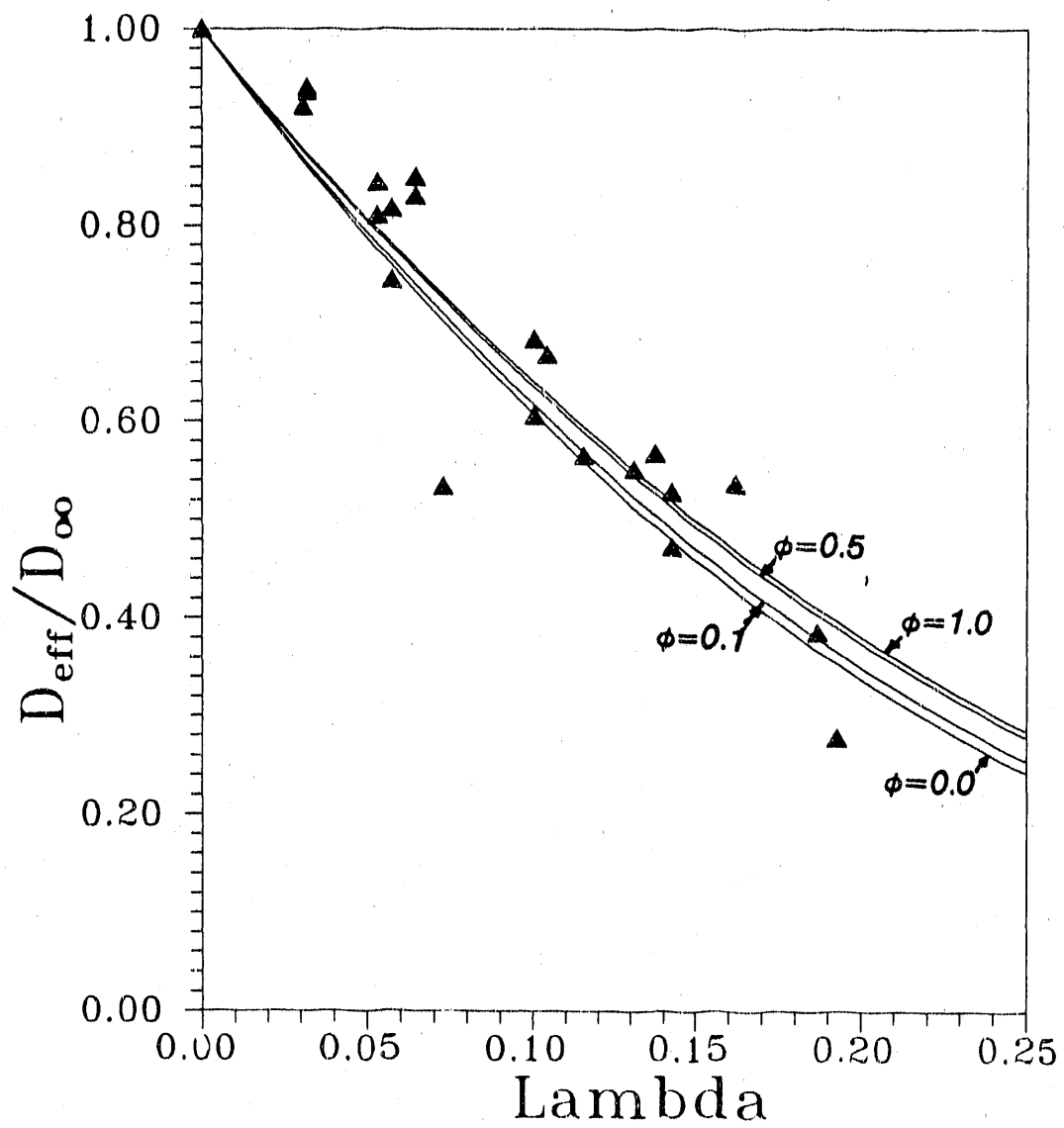Diffusion of TPP

Figure 2.   Changes in Theoretical Curve and The Hindered
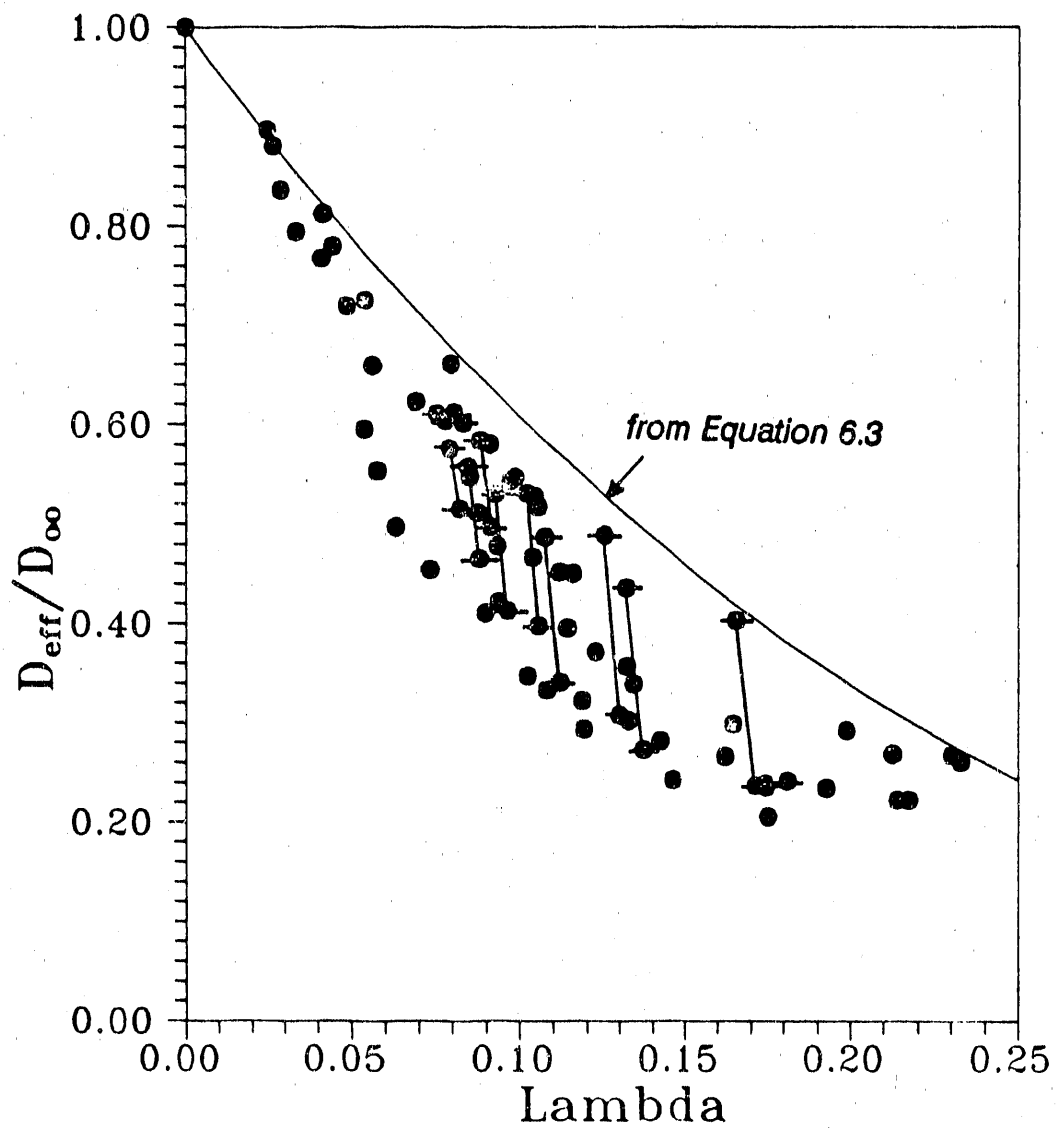   Diffusion Data of TPP

Figure 3   Dependence of D_{eff}/D_∞ on λ in Hindered
Diffusion of Coal Asphaltene

END

DATE FILMED

10 / 18 / 90